phys. stat. sol. (a) **205**, No. 2, 266–270 (2008) / **DOI** 10.1002/pssa.200723481

physica status solidi a
www.pss-a.com
applications and materials science

Deep levels associated with dislocation annihilation by Al pre-seeding and silicon delta doping in GaN grown on Si(111) substrates

C. B. Soh[**, 1], **K. Y. Zang**[1], **L. S. Wang**[1], **S. Y. Chow**[1], **and S. J. Chua**[*, 1, 2]

[1] Institute of Materials Research and Engineering, A*STAR (Agency for Science, Technology and Research), 3 Research Link, Singapore 117602, Singapore
[2] Singapore–MIT Alliance, NUS, 4 Engineering Drive 3, Singapore 11576, Singapore

Received 18 July 2007, revised 14 September 2007, accepted 4 October 2007
Published online 11 January 2008

PACS 61.72.J–, 61.72.Lk, 68.55.Ln, 71.55.Eq, 81.15.Gh

[*] Corresponding author: e-mail elecsj@nus.edu.sg
[**] e-mail cb-soh@imre.a-star.edu.sg

The introduction of Si burst during the growth of GaN film on Si(111) substrate by MOCVD formed a Si_xN_y layer which leads to an effective reduction in the density of screw dislocations. The reduction is associated with bending of screw dislocations to form a square dislocation loop when neighbouring dislocations with opposite Burger's vector paired up. The concentration of electron traps E_c-E_t ~0.17–0.26 eV which is associated with screw dislocations is substantially reduced and a kink is left at the silicon rich position. The mixed-edge dislocation, however, is not annihilated by the Si_xN_y layer. Addition of TMAl burst for the AlN growth leads to a substantial reduction in trap concentration associated with the nitrogen vacancies, V_N, and antisite of nitrogen, N_{Al}, at E_c-E_t ~0.10 eV and E_c-E_t ~ 0.60 eV respectively. This improves the quality of the subsequent layer of HT-GaN grown and is useful for device fabrication.

1 Introduction The growth of III–V nitride heterostructures on silicon substrate open up new frontier in the field of Optoelectronics as it is now possible to integrate Si electronics on the same chip. Si-based GaN LEDs [1, 2] are now commercially available and top-bottom electrode can be fabricated due to well-confined p- and n-type conductivity. However, due to the large lattice and thermal mismatched between GaN and Si [3, 4], growth of GaN film on Si substrate leads to generation of high dislocation density [5] and thermally induced cracks. The introduction of low temperature AlN multilayer [6], in-situ Si_xN_y [7, 8] masking and Si delta doping (δ-doping) [9, 10] have resulted in the significant improvement in the crystalline qualities of GaN film grown on silicon. Wang et al. [10] has reported that the addition of silicon burst for δ-doping reduces the in-plane tensile stress while Contreras et al. [9] reported the phenomenon of screw dislocation reduction. However, the electrical properties of GaN film grown on Si substrate have not been well addressed. Identification of the trap levels by deep level transient spectroscopy (DLTS) would provide more information on the characteristics of these defects. In this letter, we have investigated the influence of periodic Si delta doping on the nature of the trap levels and its relation to the dislocations and other defects in the GaN film grown on Si.

2 Experimental procedures The MOCVD growth was performed with an EMCORE D125 turbo disk reactor on Si(111) substrate. Monosilane (SiH_4) diluted in hydrogen (50 ppm) was used as Si dopants. 100 nm of AlN buffer was first deposited at 1020 °C on Si(111) substrate for 90 min in sample A, B and C. For the growth of the HT-AlN buffer, the flow rate of NH_3 and TMAl is kept at 0.45 mol/min and 200 sccm respectively with a pressure of 50 Torr. For sample B and C, it has a seed layer of Al predeposited at 1010 °C using Trimethyl Aluminium (TMAl) as the source gas for 6.0 s before the growth of the HT-AlN buffer, but not for sample A. During the growth of the

2.0 μm thick HT-GaN layer for the three samples, the flow rate of TMGa is kept at 150 μmol/min and reactor pressure maintained at 200 Torr with a temperature of 1010 °C. However, for sample C, Si periodic delta doping was done for 4 periods to form the SiN interlayers after the growth of each 0.4 μm of HT-GaN interval. The flow of TMGa was interrupted while SiH_4 was introduced at 0.167 μmol/min into the reactor for 36 s at constant NH_3 flow. The silane flow was kept at 10 sccm and this gives an estimated growth rate of 0.2 nm/s, giving a SiN interlayer of thickness ~7.0 nm. After each cycle of Si δ-doping, purging was carried out for 60 s to eliminate any memory effect in the system and to avoid residual dopants. For sample A, no Si-delta doping or TMA burst was carried out. Before conducting DLTS measurement, $C-V$ data was used to establish the carrier profile and to ascertain that the carrier concentration is much greater than the trap concentration at all temperature. Carrier concentrations $n_s \sim 5.0 \times 10^{16}$ cm^{-3}, 4.0×10^{16} cm^{-3} and 8.5×10^{16} cm^{-3} is obtained for sample A, B and C respectively.

3 Result and discussion Figure 1 shows the DLTS spectra from temperature scan from 50 K to 300 K carried out for the four samples with a period width t_w of 2.0 s under a quiescent reverse bias voltage of –2.0 V (to a depth of ~0.5 μm) and pulsed at t_p = 50 ms. Typical DLTS spectra as shown in Fig. 1(a) for the growth of undoped GaN on Si substrate gives four prominent electron traps labeled as A_1, A_2, A_4 and A_5 with energy position at $E_c-E_t \sim 0.10$ eV, 0.17 eV, 0.45 eV and 0.60 eV. The A_1 level would be related to that of the nitrogen vacancies as the activation energy for these donors found from Hall measurement, $E_D \sim 70$ meV. The discrepancy in the value is partially accounted to the error in the fitting of the Arrhenius plot. The well-defined spectra peak, A_5 at $E_c-E_t \sim 0.60$ eV has been reported to be related to nitrogen antisite N_{Ga}, in GaN grown on sapphire [11]. In sample B, with a seed layer of Al pre-deposited at 1010 °C by the TMA burst, it was observed that A_5 level has been effectively quenched from the peak spectra in Fig. 1(b). There is

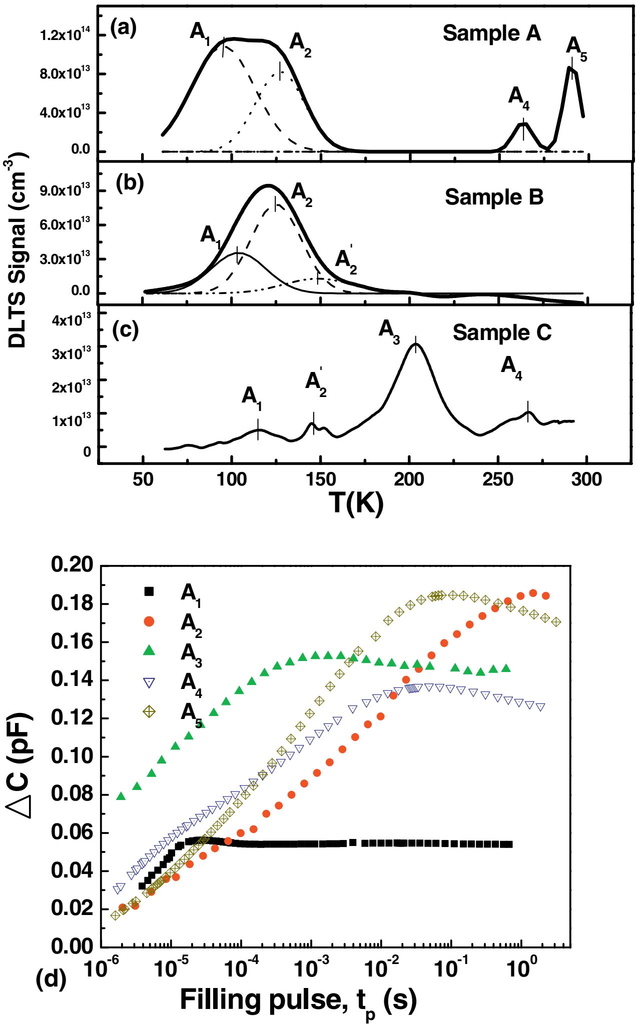

Figure 1 (online colour at: www.pss-a.com) DLTS spectra for temperature scan performed on (a) sample A, GaN grown on Si, and (b) sample B, with the addition of TMAl pre-treatment before AlN buffer growth while (c) sample C includes the addition of Si δ-doping at 70 sccm. (d) DLTS peak amplitude versus the filling pulsewidth 't_p' for the trap levels observed in Si-doped GaN.

Table 1 Trap parameters for the deep levels in GaN layer grown on Si determined from the Arrhenius plot.

level	A_1	A_2	A_2'	A_3	A_4	A_5
sample A						
E_c-E_T (eV)	0.10	0.17			0.45	0.60
σ_N (cm^2)	5.7×10^{-20}	1.8×10^{-18}			8.3×10^{-18}	1.5×10^{-16}
N_T (cm^{-3})	1.1×10^{14}	9.0×10^{13}			3.0×10^{13}	7.6×10^{13}
sample B						
E_c-E_T (eV)	0.11	0.17	0.19			
σ_N (cm^2)	1.1×10^{-19}	6.5×10^{-18}	2.5×10^{-18}			
N_T (cm^{-3})	3.2×10^{13}	7.5×10^{13}	1.2×10^{13}			
sample C						
E_c-E_T (eV)	0.10		0.19	0.39	0.45	
σ_N (cm^2)	8.3×10^{-20}		5.8×10^{-18}	5.2×10^{-17}	1.3×10^{-17}	
N_T (cm^{-3})	5.3×10^{12}		5.5×10^{12}	3.6×10^{13}	1.0×10^{13}	

also a reduction in concentration of deep level A_1 which is associated with nitrogen vacancies from 1.1×10^{14} cm^{-3} to 3.2×10^{13} cm^{-3} as shown in Table 1. It is speculated that with pre-seeding of Al adatoms on Si substrate, it enhances the crystal orientation of the AlN buffer layer, with less broken bonds and also reduces the concentration of point-like intrinsic defects for instance the vacancies, V_{Al}, V_N and its antisites, N_{Al}. Complexes of $[N_{Al} + V_{Al}]$ which are dominant in conventional AlN layer are less likely to be formed [12]. In the HT-AlN buffer, the reduction in N adatoms occupying the vacant Al site to give antisite of nitrogen, N_{Al} leads to the elimination of deep level A_5 with better bond formation of Al and N adatoms in the buffer layer.

In sample C, Si δ-doping has been carried out to form Si_xN_y layer. It has been reported by Wang et al. that with Si δ-doping, better morphology has been obtained and there is a reduction in void defects [10]. In Fig. 1(c), it was observed that there is a significant reduction in concentration of deep levels, A_2 ($E_c - E_t \sim 0.15-0.17$ eV) and A_2' ($E_c - E_t \sim 0.19-0.23$ eV) with Si-delta doping where silane flow is kept at 0.167 μmol/min. It has been reported that A_2 and A_2' are related to the decoration of O_N and Si_{Ga} along the screw dislocations respectively [14]. This is based on the high thermal stability of the O_N and Si_{Ga} which can only dissociate from the dangling bonds of screw dislocations with an annealing temperature of higher than 850 °C. The deep levels also displayed extended defect-like behavior such as asymmetrical broadening with increasing filling pulse and logarithmic capture kinetic behavior [13–17]. Similar observation was noted for this deep level A_2 in our GaN sample grown on Si substrate. This implies the less availability of the dangling bonds from the threading dislocations to form bonds with Si_{Ga} and O_N antisite. On the other hand, the higher SiH_4 flow introduces a deep level, A_3 ($E_c - E_t \sim 0.36-0.39$ eV) of trap concentration $\sim 3.6 \times 10^{13}$ cm^{-3} in the GaN layer as illustrated in Fig. 1(c). This deep level is believed to be related to that of Si point defects as it displayed an exponential capture kinetic behavior.

To further study the nature of the deep levels in Si-doped GaN, the dependence of the deep levels on filling pulse time 't_p' was monitored. A saturation pulsewidth 't_p' of 1 s, 30 ms and 60 ms is obtained for A_2, A_4 and A_5 levels, respectively, as compared to 20 μs for the A_1 level, which is typical for a point-like defect [16]. The plots of peak height, ΔC, versus the filling pulsewidth, t_p, in Fig. 1(d) show that the magnitudes of A_2 levels increase linearly with the logarithm of filling pulsewidth up to 1 s. This is an indication of the nature of trap levels associated with the extended defects [14–16]. The A_3, A_4 and A_5 level has a shorter saturation pulse time and exhibit a logarithmic capture kinetic behavior only for lower pulsewidth. Its ΔC starts to decrease with further increase in t_p as the traps are filled and re-emitted. We can attribute the deep levels A_3 to Si dopant, since it is not observed in sample A and B. This accounts for its anomalous capture kinetic behavior and its low thermal stability as reported [13], which is a feature of point defects. The relation of A_4 and A_5 levels to antisite of nitrogen, N_{Ga} and N_{Al}, explains its saturation filling pulse at tens of milliseconds. On the otherhand, the deep level A_2 are related to the linear arrays of defects due to the dangling bonds along the dislocation core sites, where charge buildup governs the capture rate. The curve will only saturate at longer filling pulses ($t_p > 1$ s), when the trap levels are effectively filled. Further increase in filling pulsewidth caused all the trap levels to emit during the capture process, which accounts for the slight reduction of the DLTS peak amplitude.

Figure 2 shows the XRD Omega scan at (0002) plane carried out for the samples using Philip X-Pert HRXRD system with the diffraction peak for GaN (0002) normalized to zero. A comparison of the intensity with its width for sample A, B and C shows that the Full width half maximum (FWHM) has been effectively reduced from 0.45° to 0.29° and 0.31° with the use of the Al pre-seeding layer and Silane burst. This indicates that the defect density in the GaN layer using Al preseeding and Silane burst has been reduced and the crystal quality at the symmetry plane has been much improved. This agrees with the finding from DLTS that density of deep level A_2 and A_2' related to the decoration of O_N and Si_{Ga} along the screw-mixed dislocations have been reduced using Silane burst and Al preseeding as (0002) symmetrical plane determines the defects related to screw dislocations. The reduction in pits can be seen in the AFM images as reported by Zang et al. [18] using the same technique but on different batch of samples.

The analysis of the deep level defects in the samples suggests that the delta doping is effective in reducing the density of threading dislocations. The effectiveness in the reduction of dislocations density is further supported by comparing the weak beam TEM image taken with diffraction vector $\boldsymbol{g} = [0002]$ with images at diffraction vector $\boldsymbol{g} = [01\bar{1}0]$ along $\langle 11\bar{2}0 \rangle$ zone axis. In general, threading

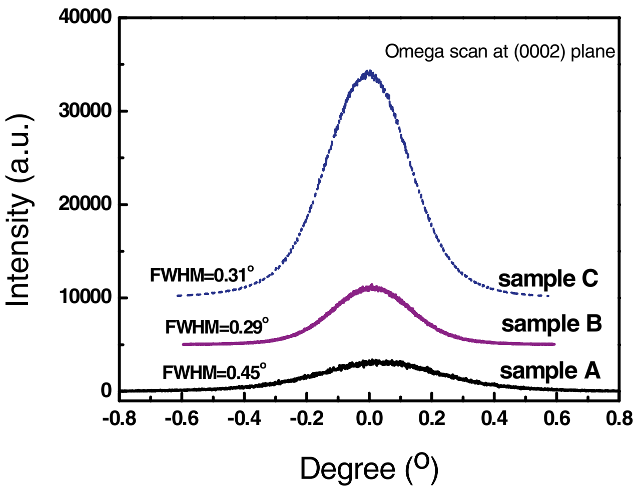

Figure 2 (online colour at: www.pss-a.com) High resolution XRD scan at (0002) plane for sample A, B and C with its x-axis normalized to zero.

dislocations which includes the screw, edge and mixed dislocations, with Burgers vectors $\boldsymbol{b} = [0001]$, $\boldsymbol{b} = 1/3[11\bar{2}0]$ and $\boldsymbol{b} = 1/3[11\bar{2}\bar{3}]$ respectively, have been observed in epitaxially grown GaN. With diffraction condition, $\boldsymbol{g} = [0002]$ as in Fig. 3(a), only screw and mixed dislocations are visible. It was observed that at Silane burst (as shown by the dotted line), the silicon atoms pin the surface step edge and forced the threading dislocation line to bend over the basal plane (as indicated by K in the figure). The screw dislocations can be paired to form a dislocation loop (L) or bends back to form a kink (K). This accounts for the substantial reduction of screw and mixed dislocations with delta doping and correlates well to the deep level analysis, where trap concentration of A_2 and A_2' decreases with Si-delta doping. With diffraction condition, $\boldsymbol{g} = [01\bar{1}0]$ as in Fig. 3(b), where only edge dislocations is shown, its density is found to be much less as compared to the screw dislocations. The edge dislocations, does not show any bending or looping and there is no substantial reduction in its density with delta doping. A number of voids (or pits) were observed at the region where silane burst was carried out. It has further been confirmed by electron energy loss spectroscopy (EELS) that Si has been incorporated in the sidewalls of these voids [18]. The different structures of these Si-rich precipitates would have account for the contrast as observed in the TEM image. With incorporation of SiN_x rich regions, large tensile stress field is developed [19] which leads to the dislocation bending as observed in Fig. 3(a).

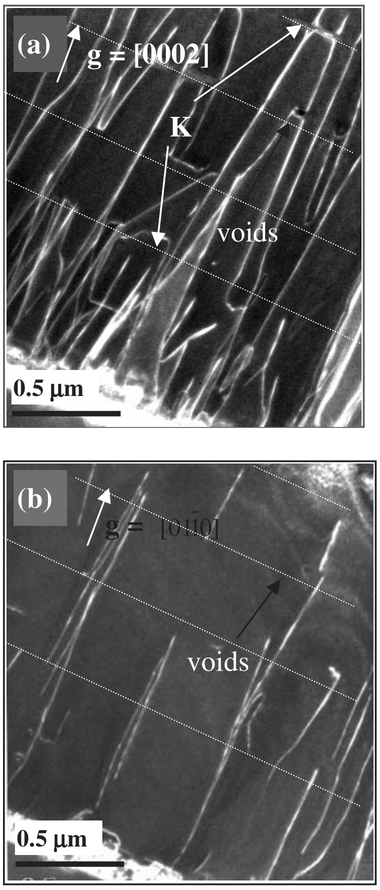

Figure 3 Weak-beam TEM images showing the effect of Si δ-doping for sample C with diffraction condition at $\boldsymbol{g} = [0002]$ for Fig. 3(a); $\boldsymbol{g} = [01\bar{1}0]$ for Fig. 3(b). The images show (a) dislocations with screw components; Burgers vectors $\boldsymbol{b} = [0002]$ and $\boldsymbol{b} = 1/3[11\bar{2}\bar{3}]$, (b) dislocations with edge component, particularly $\boldsymbol{b} = 1/3[11\bar{2}0]$. The dotted line shows the point where Si delta doping occurs and caused dislocations bending with kinks formation.

4 Conclusions

In summary, delta doping with silicon is an effective method for the reduction of the threading dislocation density (especially screw dislocations) in GaN epitaxy. The density of the deep level traps A_2 and A_2' has been much reduced with Si delta doping. TEM images show that propagation of screw dislocation has been hampered with bending and kink formation. This accounts for the reduction in the density of trap levels with energy position at $E_c - E_t \sim 0.17$ eV. The reduction in the FWHM of XRD Omega scan at (0002) plane for the Si delta doped sample with Al pre-seeding is an indication of the reduction in defect density in the GaN layer. However, the pinning by the silicon impurities of the surface lattice steps associated with screw dislocations generated a high concentration of point-like defects of Si, and leads to a substantial increase in the concentration of related traps at $E_c - E_t \sim 0.36-0.42$ eV. With pre-seeding of Al adatoms on Si substrate through TMAl burst, it enhances the crystal orientation of the AlN buffer layer and reduces the concentration of point-like intrinsic defects, the vacancies (V_N) and the antisites of nitrogen (N_{Al}) with energy position at $E_c - E_t \sim 0.10$ eV and $E_c - E_t \sim 0.60$ eV, respectively.

References

[1] J. W. Wang, A. Lunev, G. Simin, A. Chitnis, M. Shatalov, M. A. Kahn, J. E. Van Nostrand, and R. Gaska, Appl. Phys. Lett. **76**, 273 (2000).
[2] T. Egawa, B. Zhang, N. Nishikawa, H. Ishikawa, T. Jimbo, and M. Umeno, J. Appl. Phys. **91**, 528 (2000).
[3] H. Ishikawa, G. Y. Zhao, N. Nakada, T. Egawa, T. Soga, T. Jimbo, and M. Umeno, phys. stat. sol. (a) **176**, 599 (1999).
[4] A. Watanabe, T. Takeuchi, K. Hirosawa, H. Amano, K. Hiramatsu, and I. Akasaki, J. Cryst. Growth **128**, 391 (1993).
[5] S. Tanaka, Y. Kawaguchi, and N. Sawaki, Appl. Phys. Lett. **76**, 2701 (2000).
[6] A. Dadgar, J. Bläsing, A. Diez, A. Alam, M. Heuken, and A. Krost, Jpn. J. Appl. Phys. Part 2, **39**, L1183 (2000).
[7] K. J. Lee, E. H. Shin, and K. Y. Lim, Appl. Phys. Lett. **85**, 1502 (2004).
[8] A. Dadgar, M. Poschenrieder, J. Bläsing, K. Fehse, A. Diez, and A. Krost, Appl. Phys. Lett. **80**, 3670 (2002).
[9] O. Contreras, F. A. Ponce, J. Christen, A. Dadgar, and A. Krost, Appl. Phys. Lett. **81**, 4712 (2002).
[10] L. S. Wang, K. Y. Zang, S. Tripathy, and S. J. Chua, Appl. Phys. Lett. **85**, 5881 (2004).
[11] H. K. Cho, C. S. Kim, and C.-H. Hong, J. Appl. Phys. **94**, 1485 (2003).

[12] N. Yu. Arutyunov, A. V. Mikhailin, V. Yu. Davydov, V. V. Emtsev, G. A. Oganesyan, and E. E. Haller, Semiconductors **36**, 1106 (2002).
[13] C. B. Soh, S. J. Chua, H. F. Lim, D. Z. Chi, W. Liu, and S. Tripathy, J. Phys.: Condens. Matter **16**, 6305 (2004).
[14] C. B. Soh, S. J. Chua, H. F. Lim, D. Z. Chi, S. Tripathy, and W. Liu, J. Appl. Phys. **96**, 1341 (2004).
[15] D. Cavalcoli, A. Cavallini, and E. Gombia, Phys. Rev. B **56**(23), 14890 (1997).
[16] P. N. Grillot, S. A. Ringel, E. A. Fitzgerald, G. P. Watson, and Y. H. Xie, J. Appl. Phys. **77**(7), 3248 (1995).
[17] P. Omling, L. Samuelson, and H. G. Grimmeiss, J. Appl. Phys. **54**, 5117 (1983).
[18] K. Y. Zang, Y. D. Wang, L. S. Wang, S. Y. Chow, and S. J. Chua, J. Appl. Phys. **101**, 093502 (2007).
[19] F. Yun et al., J. Appl. Phys. **98**, 123502 (2005).

